Chapter 1

A case study of thermodynamic bounds for chemical kinetics

K. Proesmans

Hasselt University, B-3590 Diepenbeek, Belgium
Collège de France, 75005 Paris, France

L. Peliti

Santa Marinella Research Institute, 00058 Santa Marinella (RM), Italy

D. Lacoste [*]

Laboratoire de Physico-Chimie Théorique – UMR CNRS Gulliver 7083,
PSL Research University, ESPCI,
10 rue Vauquelin, F-75231 Paris, France

In this chapter, we illustrate recently obtained thermodynamic bounds for a number of enzymatic networks by focusing on simple examples of unicyclic or multi-cyclic networks. We also derive complementary relations which constrain the fluctuations of first-passage times to reach a threshold current.

1. Introduction

There are generally several parameters which determine the performance of a thermodynamic system. One parameter is the average output flux delivered by the system, which is related to its output power. Another parameter is the dissipation, which may be viewed as a cost for operating the system. In order for the behavior of the system to be reliable and robust, one wants small fluctuations in the output flux while at the same time a small cost of operation. These goals are generally incompatible as emphasized by a trade-off known under the name of thermodynamic uncertainty relations.[1,2] This trade-off constrains the fluctuations in product formation in enzyme

---

[*]david.lacoste@espci.fr.

kinetics[3] and can thus be used to infer information on the topology of the underlying chemical network[4,5] or to estimate the dissipation from the fluctuations of observed fluxes.[6] Suppressing fluctuations of an output flux is required to achieve some accuracy with brownian clocks,[7] while suppressing dissipation leads to an improvement in the thermodynamic efficiency of machines.[8–12] This trade-off, originally obtained for non-equilibrium steady states, holds in fact for systems at finite time[13,14] evolving in either continuous or discrete time.[15–17] It has also been adapted to Brownian motion,[18] nonequilibrium self-assembly,[19] active matter,[20] equilibrium order parameter fluctuations,[21] phase transitions,[22] first-passage-time fluctuations,[23,24] and it continues today to generate many new applications or extensions.[25–30]

In this chapter, we focus on the implications of thermodynamic uncertainty relations for chemical kinetics. We illustrate the theoretical predictions by studying particle conversion fluxes and their fluctuations for both unicyclic and multi-cyclic chemical reactions. We also show the connection with the statistics of first-passage time, defined as the first time that a given number of particles has been converted.

This review is organized as follows. In section 2, we illustrate bounds on the Fano factor for three examples of unicyclic networks, namely the isomerization reaction, the Michaelis-Menten reaction and the active catalysis. In section 3, we study one example of a multi-cylic network containing two cycles, which we call the misfolding reaction. In section 4, we study complementary relations for the fluctuations of first-passage times. We conclude in section 5.

2. Bounds for unicyclic networks

2.1. *The isomerization reaction*

Let us consider a single enzyme which can catalyze the transition between two isomers E_1 and E_2:

$$\mathrm{E}_1 \underset{k^-}{\overset{k^+}{\rightleftharpoons}} \mathrm{E}_2,$$
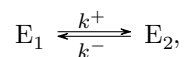
with constant transition rates k^+ and k^-. This model can be mapped on a biased random walk, with a rate of forward jumps k^+ and of backward jumps k^-. The total displacement of this walker corresponds to the difference between the number of isomers E_1 converted into E_2 minus the number of reverse conversions. The master equation of this system is given

by

$$\frac{d}{dt}P_n(t) = k^- P_{n+1}(t) - (k^+ + k^-)P_n(t) + k^+ P_{n-1}(t), \tag{1}$$

where $P_n(t)$ the probability to be at time t at the position n. The detailed balance relation takes the form

$$\frac{k^+}{k^-} = e^{\mathcal{A}}, \tag{2}$$

where $\mathcal{A}$ is the dimensionless affinity given our choice of units, $k_\mathrm{B}T = 1$.

In order to characterize the fluctuations of the variable n, we introduce the *generating function*:

$$\Psi(\lambda, t) = \sum_n e^{\lambda n} P_n(t). \tag{3}$$

Using the master equation (1), this generation function evolves according to the equation

$$\frac{d\Psi(\lambda, t)}{dt} = \theta(\lambda)\Psi(\lambda, t), \tag{4}$$

where we have defined

$$\theta(\lambda) \equiv \lim_{t \to \infty} \frac{1}{t} \ln \left\langle e^{n\lambda} \right\rangle = k^- e^{\lambda} - (k^+ + k^-) + k^+ e^{-\lambda}. \tag{5}$$

The mean and the variance of n can be expressed in terms of the derivatives of $\theta(\lambda)$ at $\lambda = 0$ as follows:

$$J = \lim_{t \to \infty} \frac{\langle n \rangle}{t} = \theta'(0) = k^+ - k^-, \tag{6}$$

$$D = \lim_{t \to \infty} \frac{\langle n^2 \rangle - \langle n \rangle^2}{2t} = \frac{\theta''(0)}{2} = \frac{k^+ + k^-}{2}. \tag{7}$$

Using these expressions, Barato *et al.*[1] have derived an "uncertainty relation" involving the following measure of the precision of the fluctuating variable n:

$$\epsilon^2 = \frac{\langle n^2 \rangle - \langle n \rangle^2}{\langle n \rangle^2} = \frac{k^+ + k^-}{(k^+ - k^-)^2 t}. \tag{8}$$

For a duration t, the total energy cost C is the product of the entropy production rate by the time t, so $C = \mathcal{A}Jt$ where J is the average conversion rate introduced above. Then the product of this cost C by the relative uncertainty ϵ^2 can be expressed by means of the detailed balance relation, Eq. (2), as

$$C\epsilon^2 = \frac{2D\mathcal{A}}{J} = \mathcal{A}\coth\left(\frac{\mathcal{A}}{2}\right) \geq 2, \tag{9}$$

where the last inequality follows from a well known property of hyperbolic tangent. Importantly, this relation expresses a trade-off between the precision quantified by ϵ and the cost quantified by C. Note that the inequality in Eq. (9) holds arbitrarily far from equilibrium, and becomes saturated only in the linear regime close to equilibrium when $\mathcal{A} \to 0$.

4   *K. Proesmans, L.Peliti and D. Lacoste*

2.2. *The reversible Michaelis-Menten reaction*

We now consider another important unicyclic network, namely the well-known Michaelis-Menten kinetics.[3] In this chemical network, a substrate S is transformed into a product P due to the presence of an enzyme E via the formation of an unstable complex ES:

$$S + E \underset{k_1^-}{\overset{k_1^+}{\rightleftharpoons}} ES \underset{k_2^-}{\overset{k_2^+}{\rightleftharpoons}} P + E,$$
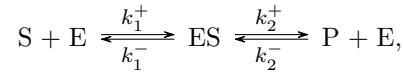
where k_1^+ is proportional to the substrate concentration and k_2^- is proportional to the product concentration. The local detailed balance relation is now given by

$$\frac{k_1^+ k_2^+}{k_1^- k_2^-} = e^{\mathcal{A}}. \tag{10}$$

We introduce $p_{\alpha,n}(t)$ as the probability to have the enzyme in the state $\alpha = 0, 1$ with $\alpha = 0$ representing the free state and $\alpha = 1$ the bound state, and with n molecules of P produced. This probability satisfies the master equations:

$$\frac{dp_{0,n}}{dt} = k_1^- p_{1,n} + k_2^+ p_{1,n-1} - (k_1^+ + k_2^-)p_{0,n}; \tag{11}$$

$$\frac{dp_{1,n}}{dt} = k_1^+ p_{0,n} + k_2^- p_{1,n+1} - (k_1^- + k_2^+)p_{1,n}. \tag{12}$$

We introduce again generating functions associated to these probability distributions by

$$\Psi_\alpha(\lambda, t) = \sum_{n=-\infty}^{+\infty} e^{\lambda(n+\alpha/2)} p_{\alpha,n}(t). \tag{13}$$

By convention a half integer value of n is assigned to states where the enzyme is bound, and a integer number when the enzyme is free. By transforming the master equation into an evolution equation for the generating function we find:

$$\frac{d}{dt}\begin{pmatrix} \Psi_0 \\ \Psi_1 \end{pmatrix} = L(z)\begin{pmatrix} \Psi_0 \\ \Psi_1 \end{pmatrix}, \tag{14}$$

with the evolution matrix

$$L(z) = \begin{pmatrix} -(k_1^+ + k_2^-) & z^{-1}k_1^- + zk_2^+ \\ zk_1^+ + z^{-1}k_2^- & -(k_1^- + k_2^+) \end{pmatrix}, \tag{15}$$

where $z = e^{\lambda/2}$. By the Perron-Frobenius theorem, there is a non-degenerate positive leading eigenvalue of L, which we denote $\theta(z(\lambda))$. Explicit evaluation of this function yields

$$J = \left.\frac{d\theta}{d\lambda}\right|_{\lambda=0} = \frac{k_1^+ k_2^+ - k_1^- k_2^-}{k_1^+ + k_1^- + k_2^+ + k_2^-}; \tag{16}$$

$$D = \frac{1}{2}\left.\frac{d^2\theta}{d^2\lambda}\right|_{\lambda=0} = \frac{k_1^+ k_2^+ + k_1^- k_2^- - 2J^2}{2(k_1^+ + k_1^- + k_2^+ + k_2^-)}. \tag{17}$$

In the context of enzymatic kinetics, the *Fano factor* characterizes the fluctuations in the formation of product by the enzyme. It is defined as

$$F = \frac{2D}{J}. \tag{18}$$

Using the above expressions for J and D together with the detailed balance condition (10) we find that

$$F = \coth\left(\frac{\mathcal{A}}{2}\right) - \frac{2k_2^- k_1^- (e^{\mathcal{A}} - 1)}{(k_2^- + k_2^+ + k_1^- + k_1^+)^2}. \tag{19}$$

A lower bound for the Fano factor can be obtained by minimizing the right-hand side of Eq. (19) with respect to all the transition rates. The minimum is obtained when $k_1^+ = k_2^+ \equiv k^+$, and $k_1^- = k_2^- \equiv k^-$. Then, using the detailed balance condition, one proves the inequality[3]

$$F \geq \frac{1}{2}\coth\left(\frac{\mathcal{A}}{4}\right) \geq \frac{2}{\mathcal{A}}. \tag{20}$$

Since the relation $C\epsilon^2 = F\mathcal{A}$ holds generally, both Eq. (9) and Eq. (20) are particular cases of a general inequality for $C\epsilon^2$ valid for a unicyclic enzyme containing N states. In their original work,[1] Barato *et al.* provided an inequality involving, $\mathcal{A}$ and N/n_c where n_c was defined as the number of consumed substrate molecules in each cycle. If one defines the Fano factor per molecule instead of per cycle, as we do here, there is no need for n_c, and the result is simpler to state: the Fano factor of a unicyclic enzyme containing N states is bounded by an expression that only depends on $\mathcal{A}$ and N:[7]

$$F \geq \frac{1}{N}\coth\left(\frac{\mathcal{A}}{2N}\right). \tag{21}$$

The example we gave previously of an isomerization reaction satisfies this relation with $N = 1$, while the Michaelis-Menten scheme does so with $N = 2$. In Fig. 1, we verify this bound by computing the Fano factor for 1000 random transition rates of the form $k_1^+ = 10^{2r_1-1}$ where r_1 is a

uniform random number in $[0,1]$, while keeping a fixed value of the affinity $\mathcal{A}$.

An affinity-independent bound follows from Eq. (21) by letting $\mathcal{A} \to \infty$[31,32]

$$F \geq \frac{1}{N}.\tag{22}$$

The limit $\mathcal{A} \to \infty$ is realized in practice as soon as one transition contributing to the affinity $\mathcal{A}$ becomes irreversible. Note that Eq. (22) can also be derived from an analysis of current fluctuations in a periodic one dimensional lattice.[33] It represents a central result of statistical kinetics, since it allows to estimate the number of states in an enzymatic cycle from measurements of fluctuations.[34]

As shown in Fig. 1, all the points are indeed above the bound $F_{\min} = 0.5$ in the case of Michaelis-Menten kinetics. In order to explore further Fano
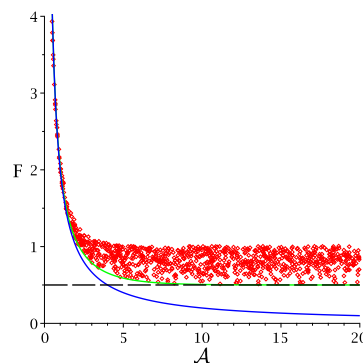

Fig. 1. The Fano factor F as a function of the affinity $\mathcal{A}$ in the Michaelis-Menten kinetics. The black horizontal dashed line represents $F_{min} = 0.5$, the blue line the bound $2/\mathcal{A}$, the green line is the hyperbolic bound of Eq. (20).

factor bounds, we now move to more complex examples.

2.3. *The active catalysis*

In this type of chemical reaction, the folding of the substrate molecule A into the product molecule B is accompanied by the hydrolysis of an ATP molecule. This reaction can be represented as a unicyclic network with four intermediate states E, E_1, E_2 and E_3 for the enzyme and two substrates A and B as shown in Fig. 2. The various reactions are
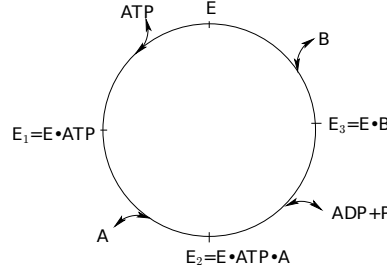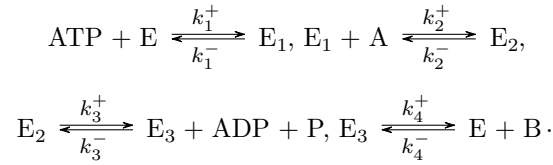
Fig. 2.   Cycle representation of the reactions involved in the active catalysis

$$\text{ATP} + \text{E} \;\underset{k_1^-}{\overset{k_1^+}{\rightleftarrows}}\; \text{E}_1,\; \text{E}_1 + \text{A} \;\underset{k_2^-}{\overset{k_2^+}{\rightleftarrows}}\; \text{E}_2,$$

$$\text{E}_2 \;\underset{k_3^-}{\overset{k_3^+}{\rightleftarrows}}\; \text{E}_3 + \text{ADP} + \text{P},\; \text{E}_3 \;\underset{k_4^-}{\overset{k_4^+}{\rightleftarrows}}\; \text{E} + \text{B} \cdot$$

The local detailed balance condition takes the form

$$\frac{k_1^+ k_2^+ k_3^+ k_4^+}{k_1^- k_2^- k_3^- k_4^-} = e^{\mathcal{A}}, \tag{23}$$

where the affinity of the cycle now reads $\mathcal{A} = \mu_A - \mu_B + \Delta\mu$, in terms of μ_A (resp. μ_B) the chemical potential of the substrate A (resp. B) and $\Delta\mu$ the chemical potential difference associated with the ATP hydrolysis reaction.

The framework of the previous section applies again here: now the evolution of the generation function is governed by a 4×4 matrix, and for this reason there is no simple analytic expression for its eigenvalues. Nevertheless, it is still possible to compute the corresponding currents and diffusion coefficients without having to obtain these explicitly by exploiting a method due to Koza as explained in Ref. [3,35]

By following this method, we obtain the plot shown in Fig. 3. As shown in this figure, the bound satisfies to the general property expected for a unicyclic enzyme given in Eq. (21) with $N = 4$ intermediate states.

3. Bounds for multi-cyclic networks: the misfolding reaction

We now switch to multi-cyclic reaction networks. As a simple example we consider the misfolding reaction, which describes an enzyme that can make errors. More precisely, the enzyme can bind a molecule A and lead to the production of the "correct" molecule, say, B, or a "wrong" one, say C. This
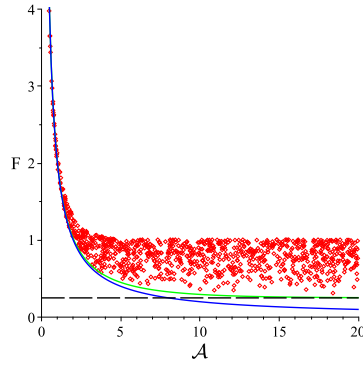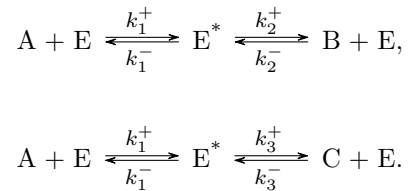
Fig. 3.   The Fano factor F as a function of the affinity $\mathcal{A}$ for the active catalyst kinetics. The black horizontal dashed line represents $F_{min} = 0.25$, the blue line the bound $2/\mathcal{A}$, the green line is the hyperbolic bound of Eq. (21) with $N = 4$.

scheme represents a network with two cycles, characterized by the same free and bound state of the enzyme. The two possible reactions that can occur are:

$$\text{A} + \text{E} \underset{k_1^-}{\overset{k_1^+}{\rightleftharpoons}} \text{E}^* \underset{k_2^-}{\overset{k_2^+}{\rightleftharpoons}} \text{B} + \text{E},$$

$$\text{A} + \text{E} \underset{k_1^-}{\overset{k_1^+}{\rightleftharpoons}} \text{E}^* \underset{k_3^-}{\overset{k_3^+}{\rightleftharpoons}} \text{C} + \text{E}.$$

We now have two different affinities driving each one of these reactions, defined by:

$$\begin{aligned}
\frac{k_1^+ k_2^+}{k_1^- k_2^-} &= e^{\mathcal{A}_1}; \\
\frac{k_1^+ k_3^+}{k_1^- k_3^-} &= e^{\mathcal{A}_2}.
\end{aligned} \tag{24}$$

The master equations describe the evolution of the probability of being in the two different enzyme states (bound and free) as a function two integer chemical variables n (resp. m), which represent the number of B (resp. C)

produced since an arbitrary time. We then have

$$
\begin{aligned}
\frac{dp_0(n,m,t)}{dt} &= k_1^- p_1(n,m,t) + k_2^+ p_1(n-1,m,t) + k_3^+ p_1(n,m-1,t) \\
&\quad - (k_1^+ + k_2^- + k_3^-)p_0(n,m,t); \\
\frac{dp_1(n,m,t)}{dt} &= k_1^+ p_0(n,m,t) + k_2^- p_0(n+1,m,t) + k_3^- p_0(n,m+1,t) \\
&\quad - (k_1^- + k_2^+ + k_3^+)p_1(n,m,t).
\end{aligned}
\tag{25}
$$

The generating function for this system can be defined by

$$
\Psi_\alpha(\overline{\lambda},t) = \sum_{n,m} e^{\overline{\lambda}\cdot(n+\alpha/2,m+\alpha/2)} p_\alpha(n,m,t),
\tag{26}
$$

where $\overline{\lambda}$ is a vector containing the two variables λ_1 and λ_2 associated to the degrees of freedom n and m respectively. The evolution matrix that governs the dynamics of the generating function is given by

$$
L(z_1,z_2) = \begin{pmatrix} -(k_1^+ + k_2^- + k_3^-) & (z_1 z_2)^{-1} k_1^- + \frac{z_1}{z_2} k_2^+ + \frac{z_2}{z_1} k_3^+ \\ z_1 z_2 k_1^+ + \frac{z_2}{z_1} k_2^- + \frac{z_1}{z_2} k_3^- & -(k_1^- + k_2^+ + k_3^+) \end{pmatrix}
\tag{27}
$$

Again, the leading eigenvalue of $L(z_1,z_2)$, called $\Theta(z_1,z_2)$, allows us to obtain the currents J_1 and J_2 and their diffusion coefficients D_1 and D_2.

Using these parameters, we can compute two Fano factors F_1 and F_2, defined by $F_i = 2D_i/J_i$, where $i = 1, 2$. Similarly, we define the corresponding cost-fluctuations parameters $C\epsilon_i^2 = F_i\Sigma/J_i$, which instead contain the total entropy production rate $\Sigma = \mathcal{A}_1 J_1 + \mathcal{A}_2 J_2$.

The error-cost parameters $C\epsilon_i^2$ are constrained by the uncertainty relation[3] :

$$
C\epsilon_i^2 \geq \frac{\bar{\mathcal{A}}}{2} \coth\left(\frac{\bar{\mathcal{A}}}{4}\right) \geq \max(2, \frac{\bar{\mathcal{A}}}{2}),
\tag{28}
$$

where $\bar{\mathcal{A}}$ is the minimum of the two cycle affinities $\mathcal{A}_1$ and $\mathcal{A}_2$.

We have verified numerically this inequality in the left panel of Fig. 4, which was constructed by generating randomly transition rates for 5000 iterations and then evaluating the error-cost parameters and the two different cycle affinities $\mathcal{A}_1$ and $\mathcal{A}_2$ using the detailed balance conditions (24).

In this case where the affinities $\mathcal{A}_1$ and $\mathcal{A}_2$ differ, we observe that a bound of the form of Eq. (21) does not hold in general for the two Fano factors F_i in terms of the affinities $\mathcal{A}_i$ or $\bar{\mathcal{A}}$. In contrast to that, the two Fano factors F_i are always bounded by $1/2$, which is the limit expected for unicycles with $N = 2$ states. This confirms that the bound in $1/N$ for the
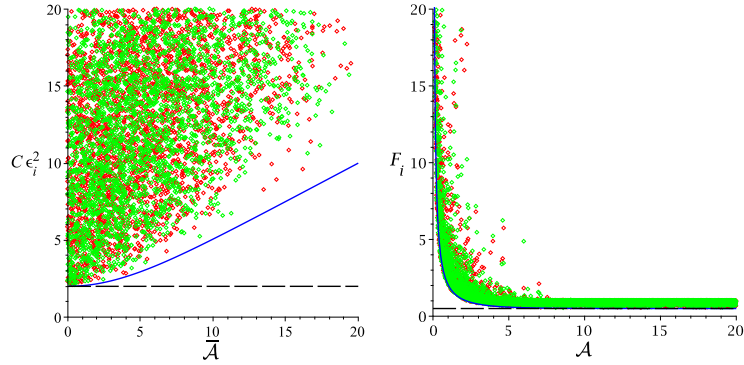
Fig. 4. Left: Error-cost parameters $C\epsilon_i^2$ as a function of the minimum $\bar{\mathcal{A}}$ of the two different affinities $\mathcal{A}_1$ and $\mathcal{A}_2$ of the two cycles. The blue solid and black dashed line illustrate the bound of Eq. (28). Right: Fano factor F_i as function of the single affinity $\mathcal{A} = \mathcal{A}_1 = \mathcal{A}_2$. The blue solid and black dashed line illustrate the bound of Eq. (21). In both figures, red points represent $i = 1$ and green points $i = 2$.

Fano factor—a central result in statistical kinetics—holds in general and is not just a consequence of the thermodynamic uncertainty relation.

In the particular case where the two affinities $\mathcal{A}_1$ and $\mathcal{A}_2$ are equal, then the bound of the form of Eq. (21) holds again for the two Fano factors F_i as shown in the right panel of Fig. 4. Thus, we have illustrated the bound for the error-cost parameter which is linked to the the uncertainty relation, but importantly we find that no affinity dependent bound of this type exist for the two Fano factors except in the particular case where all the cycles have the same affinity.

4. Bound on the fluctuations of first-passage times

The Fano factor bounds derived above represent a general property of current fluctuations probed for a fixed observation time. It is also interesting to look at these results from a different point of view, which focuses instead on fluctuations of first-passage times to reach a threshold of time-integrated current.[24]

In this section, we derive the corresponding relations for the examples we have studied above. We rely on the so-called renewal equation to analyze first-passage times for Markovian jump processes. This equation connects the propagator $p(n, t)$, *i.e.*, the probability of being in n at time t given that one starts from 0 at time 0, to the probability $F(n, t)$ to reach the

state n for the first time at time t [36, p. 307]:

$$p(n,t) = \delta_{n,0}\delta_{t,0} + \int_0^t d\tau \, F(n,\tau)p(0,t-\tau), \tag{29}$$

where one assumes that the initial state is at $n = 0$ and that the process is translation invariant. Taking the Laplace transform of this equation gives

$$\tilde{F}(n,s) = \frac{\tilde{p}(n,s)}{\tilde{p}(0,s)}, \tag{30}$$

with $\tilde{F}(n,s)$ (resp. $\tilde{p}(x,s)$) the Laplace transforms of $F(n,t)$ (resp. $p(n,t)$). Since $\tilde{F}(x,s)$ is the moment generating function of the first-passage time to reach n, which we now denote T, the first and second cumulants of T are:

$$\langle T \rangle = -\left.\frac{d}{ds}\ln\left(\tilde{F}(n,s)\right)\right|_{s=0}, \qquad \text{Var}(T) = \left.\frac{d^2}{ds^2}\ln\left(\tilde{F}(n,s)\right)\right|_{s=0}. \tag{31}$$

The connection between current fluctuations probed for a fixed observation time and first-passage times fluctuations goes in fact beyond the first and second moments. Indeed, let us evaluate the cumulant generating function of the first-passage time T:

$$g(s) = \lim_{n\to\infty}\frac{1}{n}\ln\left\langle e^{-sT}\right\rangle = \lim_{n\to\infty}\frac{1}{n}\ln\tilde{F}(n,s) \tag{32}$$

One can then show that $g(s)$ is related to the cumulant generating function of the flux of n, which is the function we have denoted earlier by $\theta(s)$, by the following relation:[24]

$$g(s) = \theta^{-1}(s). \tag{33}$$

4.1. *Isomerization relation*

Let us now verify these new relations, starting with the isomerization reaction. In this case, the equation obtained by Laplace transforming the master equation Eq. (1) admits a solution of the form $\tilde{p}_n(s) = \mathcal{N}\lambda(s)^n$ when $W^+ \geq W^-$ and $n \geq 0$, with

$$\lambda(s) = \frac{s + W^+ + W^- - \sqrt{(s + W^+ + W^-)^2 - 4W^+W^-}}{2W^+}. \tag{34}$$

Using Eq. (30), one obtains $\tilde{F}(n,s) = \lambda(s)^n$. Then with Eq. (31), one finds

$$\langle T \rangle = \frac{n}{W^+ - W^-}, \qquad \text{Var}(T) = \frac{n(W^+ + W^-)}{(W^+ - W^-)^3}. \tag{35}$$

We recall that the energy cost C is related to the entropy production rate Σ by $C = t\Sigma = \mathcal{A}Jt$, with the affinity $\mathcal{A}$ defined in Eq. (2) and the average

current J defined in Eq. (6). Then, one obtains the uncertainty relation complementary to Eq. (9):

$$\Sigma \frac{\text{Var}(T)}{\langle T \rangle} = \mathcal{A} \coth\left(\frac{\mathcal{A}}{2}\right) \geq 2. \tag{36}$$

This relation means that fluctuations in first-passage times can be reduced only at the price of an increase of dissipation. Note that fluctuations of first-passage times are not constrained by dissipation when $W^+ \leq W^-$, because in this case the mean first-passage time is infinite.

The relation between the generating functions of first-passage time and current is also easily verified. Indeed, since $\tilde{F}(n, s) = \lambda(s)^n$,

$$g(s) = \ln \lambda(s). \tag{37}$$

Then, from the definition of the cumulant generating function of n introduced in Eq. (4), one finds

$$s = \theta[\theta^{-1}(s)] = W^+ e^{\theta^{-1}(s)} + W^- e^{-\theta^{-1}(s)} - (W^+ + W^-), \tag{38}$$

therefore

$$\theta^{-1}(s) = \ln\left(\frac{s + W^+ + W^- - \sqrt{(s + W^- + W^+)^2 - 4W^- W^+}}{2W^+}\right), \tag{39}$$

which is clearly equivalent to plugging Eq. (34) into Eq. (37) in agreement with Eq. (33).

4.2. *Michaelis-Menten reaction*

The first-passage time uncertainty relation can be validated in an analogous way for the Michaelis-Menten reaction. We first need to determine $\tilde{p}_{0/1,n}(n, s)$. This can be done by taking the Laplace transform of Eq. (12):

$$(s + k_1^+ + k_2^-)\tilde{p}_{0,n} = k_1^- \tilde{p}_{1,n} + k_2^+ \tilde{p}_{1,n-1}, \tag{40}$$

$$(s + k_1^- + k_2^+)\tilde{p}_{1,n} = k_1^+ \tilde{p}_{0,n} + k_2^- \tilde{p}_{0,n+1}. \tag{41}$$

Along the lines of the isomerization reaction, we assume that $\tilde{p}_{0/1,n}(s) = \mathcal{N}_{0/1}\lambda(s)^n$, leading to

$$\lambda(s) = \frac{s^2 + Ks + k^+ + k^- - \sqrt{(s^2 + Ks + k^+ + k^-)^2 - 4k^+ k^-}}{2k^-}, \tag{42}$$

where we have introduced

$$K = k_1^+ + k_2^+ + k_1^- + k_2^-, \qquad k^- = k_1^- k_2^-, \qquad k^+ = k_1^+ k_2^+ \tag{43}$$

to simplify notations. This again leads to the first two cumulants:

$$\langle T \rangle = \frac{Kn}{k^+ - k^-}, \qquad \mathrm{Var}(T) = \frac{\left(K^2(k^+ + k^-) - 2(k^+ - k^-)^2\right)n}{(k^+ - k^-)^3}. \quad (44)$$

The thermodynamic uncertainty relation for first-passage times, Eq. (36) can now be verified easily.

As mentioned before, the cumulant generating function associated with the first-passage time is given by $g(s) = \ln\lambda(s)$, where $\lambda(s)$ is given by Eq. (42). One can invert this expression to determine the cumulant generating function $\theta(\mu)$ associated with the number of produced particles:

$$\theta(s) = g^{-1}(s) = \frac{\sqrt{K^2 + 4(e^s - 1)(k^- - k^+ e^{-s})} - K}{2} \quad (45)$$

4.3. *Misfolding reaction*

As a final example, we shall now turn to the misfolding reaction. This reaction network can be decomposed into two independent fluxes: the production of B molecules and the production of C molecules. Let us focus on the first-passage time to produce n molecules of B type. This problem can be mapped on the Michaelis-Menten reaction: indeed B is produced from E^* at a rate k_2^+ and produces E^* at a rate k_2^-. On the other hand, E^* is constructed from some other source (either A or C) at the rate $k'^+_1 = k_1^+ + k_3^-$ and deconstructed at rate $k'^-_1 = k_1^- + k_3^+$. Therefore the system can be mapped onto a Michaelis-Menten system with k_1 replaced by k'_1. One concludes that Eqs. (42–44) also hold for the misfolding reaction, with the appropriate change of rates. Using the expression for the entropy production rate Σ determined in Section 3, leads to the thermodynamic uncertainty relation in the form:

$$\Sigma \frac{\mathrm{Var}(T)}{\langle T \rangle} \geq 2. \quad (46)$$

5. Conclusion

In this chapter, we have illustrated a number of thermodynamic bounds for chemical kinetics and particularly for chemical cycles. In both unicyclic and multicyclic networks, we have confirmed the thermodynamic uncertainty relation which limits the precision that a chemical system can achieve for a given cost in terms of chemical dissipation. We have pointed out that only in unicyclic networks or in multicyclic networks subjected to a single affinity, there is a simple affinity dependent bound. In contrast to that,

K. Proesmans, L.Peliti and D. Lacoste

there is always an affinity independent bound for the Fano in terms of the inverse number of states, but this bound does not contain any trade-off.

Very recently, Gingrich and Horowitz reported a relation between the large deviation functions for currents and first-passage times in general Markov chains.[24] They also made an interesting connection between the thermodynamic uncertainty relation and first-passage time statistics. In this chapter, we have also verified their result on our examples. In future work, we would like to explore this connection further, because it could be used in both ways: on one hand one could gain insights into currents fluctuations using results on first-passage time statistics and on the other hand one can understand better first-passage time statistics using large-deviation techniques, originally introduced for the analysis of current fluctuations in non-equilibrium systems.

Acknowledgments

References

1. A. C. Barato and U. Seifert, Thermodynamic uncertainty relation for biomolecular processes, *Phys. Rev. Lett.* **114**, 158101 (Apr, 2015).
2. T. R. Gingrich, J. M. Horowitz, N. Perunov, and J. L. England, Dissipation bounds all steady-state current fluctuations, *Phys. Rev. Lett.* **116**, 120601 (Mar, 2016).
3. A. C. Barato and U. Seifert, Universal bound on the Fano Factor in enzyme kinetics, *J. Phys. Chem. B.* **119**(22), 6555–6561 (Jun, 2015).
4. P. Pietzonka, A. C. Barato, and U. Seifert, Universal bounds on current fluctuations, *Phys. Rev. E.* **93**(5), 052145 (May, 2016).
5. P. Pietzonka, A. C. Barato, and U. Seifert, Affinity- and topology-dependent bound on current fluctuations, *J. Phys. A-Math. Gen.* **49**(34), 34LT01 (2016).
6. T. R. Gingrich, G. M. Rotskoff, and J. M. Horowitz, Inferring dissipation from current fluctuations, *J. Phys. A-Math. Gen.* **50**(18), 184004 (2017).
7. A. C. Barato and U. Seifert, Cost and precision of brownian clocks, *Phys. Rev. X.* **6**, 041053 (Dec, 2016).
8. P. Pietzonka, A. C. Barato, and U. Seifert, Universal bound on the efficiency of molecular motors, *J. Stat. Mech.* **2016**(12), 124004 (2016).
9. M. Polettini, A. Lazarescu, and M. Esposito, Tightening the uncertainty principle for stochastic currents, *Phys. Rev. E.* **94**, 052104 (Nov, 2016).

Thermodynamic bounds for chemical kinetics   15

10. C. Maes, Frenetic bounds on the entropy production, *Phys. Rev. Lett.* **119** (16), 160601 (2017).

11. W. Hwang and C. Hyeon, Energetic costs, precision, and transport efficiency of molecular motors, *J. Phys. Chem. Lett.* (2018).

12. H. Vroylandt, D. Lacoste, and G. Verley, Degree of coupling and efficiency of energy converters far-from-equilibrium, *J. Stat. Mech.* p. 023205 (2018).

13. P. Pietzonka, F. Ritort, and U. Seifert, Finite-time generalization of the thermodynamic uncertainty relation, *Phys. Rev. E.* **96**(1), 012101 (2017).

14. J. M. Horowitz and T. R. Gingrich, Proof of the finite-time thermodynamic uncertainty relation for steady-state currents, *Phys. Rev. E.* **96**, 020103 (Aug, 2017).

15. S. Pigolotti, I. Neri, É. Roldán, and F. Jülicher, Generic properties of stochastic entropy production, *Phys. Rev. Lett.* **119**(14), 140604 (2017).

16. K. Proesmans and C. Van den Broeck, Discrete-time thermodynamic uncertainty relation, *Europhys. Lett.* **119**(2), 20001 (2017).

17. D. Chiuchiù and S. Pigolotti, Mapping of uncertainty relations between continuous and discrete time, *arXiv preprint arXiv:1711.00615* (2017).

18. C. Hyeon and W. Hwang, Physical insight into the thermodynamic uncertainty relation using brownian motion in tilted periodic potentials, *Phys. Rev. E.* **96**(1), 012156 (2017).

19. M. Nguyen and S. Vaikuntanathan, Design principles for nonequilibrium self-assembly, *Proc. Natl. Acad. Sci. U.S.A.* **113**(50), 14231–14236 (2016).

20. G. Falasco, R. Pfaller, A. P. Bregulla, F. Cichos, and K. Kroy, Exact symmetries in the velocity fluctuations of a hot brownian swimmer, *Phys. Rev. E.* **94**, 030602 (Sep, 2016).

21. J. Guioth and D. Lacoste, Thermodynamic bounds on equilibrium fluctuations of a global or local order parameter, *Europhys. Lett.* **115**(6), 60007 (2016).

22. A. P. Solon and J. M. Horowitz, Phase transition in protocols minimizing work fluctuations, *arXiv preprint arXiv:1712.05816* (2017).

23. J. P. Garrahan, Simple bounds on fluctuations and uncertainty relations for first-passage times of counting observables, *Phys. Rev. E.* **95**(3), 032134 (2017).

24. T. R. Gingrich and J. M. Horowitz, Fundamental bounds on first passage time fluctuations for currents, *Phys. Rev. Lett.* **119**, 170601 (Oct, 2017).

25. G. M. Rotskoff, Mapping current fluctuations of stochastic pumps to nonequilibrium steady states, *Phys. Rev. E.* **95**(3), 030101 (2017).

26. A. Dechant and S.-i. Sasa, Current fluctuations and transport efficiency for general Langevin systems, *arXiv preprint arXiv:1708.08653* (2017).

27. K. Brandner, T. Hanazato, and K. Saito, Thermodynamic bounds on precision in ballistic multiterminal transport, *Physical review letters.* **120**(9), 090601 (2018).

28. S. K. Manikandan and S. Krishnamurthy, Exact results for the finite time thermodynamic uncertainty relation, *J. Phys. A-Math. Gen.* (2018).

29. H. Wierenga, P. R. t. Wolde, and N. B. Becker, Quantifying fluctuations in reversible enzymatic cycles and clocks, *arXiv preprint arXiv:1801.05392*

16   *K. Proesmans, L.Peliti and D. Lacoste*

(2018).

30. A. Dechant and S. Sasa, Entropic bounds on currents in langevin systems, *arXiv preprint arXiv:1803.09447* (2018).

31. J. R. Moffitt, Y. R. Chemla, and C. Bustamante, Mechanistic constraints from the substrate concentration dependence of enzymatic fluctuations, *Proceedings of the National Academy of Sciences.* **107**(36), 15739–15744 (2010).

32. G. Knoops and C. Vanderzande, On the motion of kinesin in a viscoelastic medium, *arXiv preprint arXiv:1710.07151* (2017).

33. B. Derrida, Velocity and diffusion constant of a periodic one-dimensional hopping model, *J. Stat. Phys.* **31**, 433 (1983).

34. J. R. Moffitt and C. Bustamante, Extracting signal from noise: kinetic mechanisms from a Michaelis-Menten like expression for enzymatic fluctuations, *FEBS J.* **281**, 498 (2014).

35. Z. Koza, Maximal force exerted by a molecular motor, *Physical Review E.* **65**(3), 031905 (2002).

36. N. Van Kampen, *Stochastic Processes in Physics and Chemistry.* North-Holland Personal Library (2007).